Title
RELAXATION AND FINAL-STATE STRUCTURE IN XPS OF ATOMS, MOLECULES, AND METALS

Authors
Shirley, D.A.
Martin, R.L.
McFeely, F.R.
et al.

Publication Date
1975-03-01

To be presented at the Electron
Spectroscopy of Solids and Surfaces,
Vancouver, Canada, July 15 - 17, 1975

LBL-3476
c.1

RELAXATION AND FINAL-STATE STRUCTURE IN XPS OF ATOMS, MOLECULES, AND METALS

D. A. Shirley, R. L. Martin, F. R. McFeely,
S. P. Kowalczyk, and L. Ley

March 1975

Prepared for the U. S. Atomic Energy Commission
under Contract W-7405-ENG-48

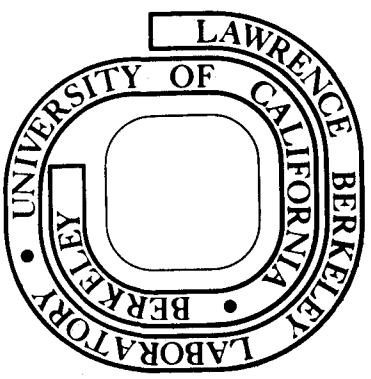

LBL-3476
c.1

DISCLAIMER

RELAXATION AND FINAL-STATE STRUCTURE IN XPS OF ATOMS, MOLECULES, AND METALS*

D.A.Shirley, R.L.Martin, F.R.McFeely, S.P.Kowalczyk, and L.Ley

Department of Chemistry and
Lawrence Berkeley Laboratory
University of California
Berkeley, California 94720

ABSTRACT: Photoemission from a many-electron system is a many-electron process, even though the transition operator may affect only one electron directly. Relaxation and "shake-up" structure are related by a sum rule. When one is present, the other must be also. Shake-up structure is shown to be accurately predictable in atomic neon and molecular HF if the CI calculations are done carefully. In metals the sum rule also applies but final-state effects usually appear as relaxation energy, which is large even for valence electrons. Finally, in rare-earth metals discrete shake-up structure is observable in the 4p region.

1. INTRODUCTION

Photoelectron spectroscopy has progressed well beyond the one-electron approximation. Nevertheless, much of our common parlance on the subject involves expressions such as "relaxation" and "shake-up" derived from one-electron pictures. In this paper we discuss photoemission spectra from a more general viewpoint, emphasizing the relation between relaxation and shake-up and the fundamental similarity in this regard of atoms, molecules, and solids. Section 2 deals with the accurate calculation of shake-up energies and intensities in atoms and molecules. Metals are discussed in Section 3, and data showing shake-up structure in rare-earth 4p spectra are presented in Section 4.

2. ATOMS AND MOLECULES

The photoelectron spectrum of an atomic or molecular species yields information about its various ionic states. Although in principle there is an infinite manifold of such states, the cross section for photoionization discriminates against all but a few. Generally speaking, a comparison of the electronic structure of the ionic state to that of the ground state permits the identification of "primary" ionic states and "satellites".

The primary states usually correspond to the most intense peaks in the spectrum and are those directly related to Koopmans' description of photoionization.[1] They thus provide very direct information about the shell structure of the ground state. Koopmans' frozen-orbital ionic state is not, however, a true many-electron eigenstate of the Hamiltonian. The electron density in the eigenstate has actually rearranged. The stabilization afforded by this relaxation reduces the binding energy from that predicted by Koopmans' Theorem.[2] Even though relaxation is an artificial concept which arises when we compare the actual final state to an approxiation to it, the fact that Koopmans' assumption represents a well defined first approximation

(and a rather good one) makes it useful. Relaxation can then be envisioned as a secondary process whereby the other electrons react to the influence of the departure of the photoelectron.[3]

Satellite peaks appear on the high binding energy side of each core-level primary peak. The most intense of these correspond to states which can be imagined as being reached by a simultaneous core orbital ionization and (monopole) valence electron excitation. The reason for this monopole "selection rule" is that to a first approximation the transition moment to such a state is dictated by the overlap integral between the valence orbital in the initial-state and the final-state orbital which the electron is "shaken up to". Once again it is the total wavefunction of the state which is meaningful and this orbital picture is just a helpful approximation. If the total wavefunction of the final state has a component which connects it with the initial state via the transition operator, it will be observed. It may be that this component is not adequately described in a one-electron picture, and in fact satellites have been observed which appear to involve a dipole excitation of a valence electron,[4,5] two-electron excitations relative to the primary state,[6,7] etc.

Recent work on the relative intensities of F 1s satellites in the hydrogen fluoride molecule[8,9] has shown the importance of configuration interaction effects in determining quantitative cross-section ratios. The HF molecule in its ground state is described by the Hartree-Fock configuration $1\sigma^2 2\sigma^2 3\sigma^2 1\pi^4$, with the F 1s hole state represented by the single configuration $1\sigma^1 2\sigma^2 3\sigma^2 1\pi^4$. The particular model used to obtain shake-up states employs a configuration expansion technique. One chooses a set of configurations which are expected to approximate closely the structure of the excited state. In the HF case these would be

$$1\sigma^1 2\sigma^2 3\sigma^1 4\sigma^1\ 1\pi^4 \quad ; \quad 1\sigma^1 2\sigma^2 3\sigma^2\ 1\pi^3 2\pi$$

$$1\sigma^1 2\sigma^2 3\sigma^1 5\sigma^1\ 1\pi^4 \quad ; \quad 1\sigma^1 2\sigma^2 3\sigma^2\ 1\pi^3 3\pi$$

$$\vdots \qquad\qquad\qquad \vdots$$

For each of these configurations two linearly-independent configuration state functions of $^2\Sigma^+$ symmetry can be formed. The Hamiltonian matrix in this configuration basis -- using, for example, the orbitals optimized for the F 1s hole state -- is formed and diagonalized. The lowest root of this CI matrix will be predominantly the F 1s hole state configuration, while the higher roots should be fairly good approximations to the shake-up states. These higher roots are usually dominated by two or three configuration state functions and can be interpreted as being reached by either a particular excitation or possibly a small number of one-electron excitations. The relative intensities are then computed in the overlap approximation.[8,10] The effective intensity of the final-state is given simply by the overlap integral between the final-state CI wavefunction and an initial-state in which the 1σ electron has been annihilated.

The results of this approach are compared to experiment in the column labeled Method A in Table 1. Although the general appearance of the spectrum is reproduced, nearly all the intensities are predicted to be a factor of two weaker than the experimental result. The reason for this lies in the fact that we have used a single determinantal initial-state; components in the true many-electron initial-state which contribute substantially to the satellite intensities are not described by the Hartree-Fock function. The results obtained using a correlated initial-state wavefunction (Method B in Table 1) are in essentially quantitative agreement with experiment.

We are presently using this model to predict the satellite intensities in the Ne 1s hole-state satellite spectrum. Preliminary results using the analog of Method A are shown in Table 2. An examination of this table shows that the overall appearance of the spectrum is predicted quite nicely. The intensities relative to the primary hole-state are once again too small.[12a] We are currently examining possible causes for the low theoretical intensities. Because the satellites are

very weak, additional small configuration-interaction effects in both the final- and initial-states could have important consequences for the computed intensities.

The intensities of the satellite peaks associated with a given primary state are related to the relaxation energy in the primary state through an approximate sum rule derived by Manne and Åberg:[13]

$$E_R = \frac{\sum_{i=1}^{\infty} (I_i/I_o)\Delta_i}{\sum_{i=0}^{\infty} (I_i/I_o)} \qquad (2.1)$$

Here E_R is the relaxation energy, (I_i/I_o) is the intensity of the satellite peak relative to the primary peak, and Δ_i is the energy separation between the satellite and the primary peak. The summations are taken over all the discrete states; they convert to an integration over any continua. The denominator simply reflects a normalization condition.

This expression should be rather precise for the core-level peaks observed in conventional XPS experiments using soft x-rays ($h\nu \approx 1.5$ keV). In principle, everything on the right hand side of Eq. (2.1) is experimentally observable, and the sum rule provides the apparatus for determining the relaxation energy without specific recourse to a Hartree-Fock calculation. In practice the relationship is not too useful in this respect because the intensity distribution of the "shake-off" continuum is not readily deduced from the spectrum. Nevertheless, the sum rule can provide a great deal of qualitative information about the photo-emission process. Equation (2.1) expresses a "lever-arm" relationship. A given value of E_R can be manifested as intense satellites near the primary peak, weak satellites distant from the primary peak, a broad continuum of satellites on the high binding energy side of the primary peak, etc.

3. METALS

Turning from small molecules to metals, we should first emphasize that there is no fundamental difference between an isolated metal crystal and a molecule in the gas phase. Therefore, all the above conclusions reached about molecular photoemission hold equally true for the metal crystal. The language of molecular theory is, however, somewhat inappropriate for discussing metals, instead, solid-state theory which deals with a hypothetical substance, the infinite crystal, must be employed.

While one can argue formal equivalency of the small molecule and the crystal, the high symmetry and macroscopic extent of the crystal result in some qualitatively different effects. The most notable of these is the occurrence of plasmons, elementary collective excitations of the valence electron gas, without analog in small molecules. In addition, the valence-electron canonical orbitals extend over the entire crystal, and their energy spacing is nearly continuous, yielding an immense number of nearly degenerate "configurations". We shall treat photoemission from core-states and band-states separately.

3.1 Core Levels

Figure 1 shows a typical spectrum of a core level. We note the following features:

1) an asymmetric primary peak at considerably lower binding energy (with respect to the vacuum level) than in the free atom,
2) a flat, constant tail to higher binding energy, and
3) one or more surface and bulk plasmon peaks.

This loss structure, in contrast to that observed in the gas phase, all results from the total process of electron emission from the crystal. While all of these peaks may in principle be treated on an equal footing, we shall, following common practice, treat photoemission by a semiclassical three-stage model:

1) optical excitation

2) transport to the surface, and

3) escape into the vacuum.

This model, as Mahan[14] and Fiebelman and Eastman[15] have shown, may be derived from a Golden Rule expression for photoemission. It has the desirable property of separating the one-electron band-structure effects from the many-body and surface effects. We shall deal primarily with step 1) of the process.

The difference in binding energies between free atom and metallic core levels implies the existence of an extra-atomic relaxation energy. Hedin and Johansson[16] have shown that the binding energy for an atomic electron in orbital $|i\rangle$ is given by

$$E_B^{(i)}(\text{atom}) \cong -\varepsilon_i - \tfrac{1}{2}\langle i | V_p^a | i \rangle \tag{3.1}$$

where ε_i is the orbital energy and V_p^a is the "polarization potential" given by

$$V_p^{(a)} = V_a^* - V_a \quad , \tag{3.2}$$

the difference in the total Hartree-Fock potentials for the ion and atom. Similarly, for a metal we can express the binding energy as

$$E_B^i(\text{metal}) = -\varepsilon_i - \tfrac{1}{2}\langle i | V_p^a | i \rangle - \tfrac{1}{2}\langle i | V_p^{ea} | i \rangle \tag{3.3}$$

The extra-atomic polarization potential, V_p^{ea}, is appreciable because a semi-localized state has formed around the ion from the bottom of the valence bands, self-consistently screening the core hole from the lattice (analogous to Friedel alloy theory).[17] We approximate V_p^{ea} by the Hartree-Fock potential of the atomic orbital out of which the lowest conduction band state is formed. Since hole-state calculations on the final-state ions [necessary for the calculation

of $(V^* - V)]$ are unavailable, we approximate the coulomb and exchange integrals necessary to evaluate $\langle i \mid V_p^{ea} \mid i \rangle$ by an equivalent cores approximation. The result for the 3d transition series is shown in Figure 2. Note that the model represents an overestimate, since the screening charge is not localized as an atomic state but rather semi-localized.

Since there is clearly relaxation in the core-level spectra, one expects to find "shake-up structure". One of these effects is the asymmetry exhibited by core level lines.[18,19] This effect was considered first by Mahan,[20] Anderson[21] and others. It arises from the coupling between the core-hole and valence-band electron-hole pairs. In the language of molecular theory, a configuration with an excited electron-hole pair in the valence band couples with the "primary" hole-state without these excitations and acquires intensity from it. A discussion of the quantitative measure of the asymmetry and its comparison with theoretical predictions is given by Ley et al.[22]

In addition to coupling to configurations with excited electron-hole pairs, several workers[23,24] have described the coupling between the primary hole-state and plasmons in the valence electron gas. This results in the appearance of satellite peaks at higher binding energy at integral multiples of the plasmon energy. However, all of the plasmon peaks observed in the XPS spectra[25] do not represent the intensity predicted by the Lundqvist and Langreth theories and the intensity sum rule. In fact, the sum rule is not very useful for solids, a point which may be appreciated by considering the total states of the N-particle system. The photoemission process may be written as

$$\psi^N_{\text{GROUND STATE}} + \text{photon} \rightarrow \psi^N_{\text{EXCITED}} ,$$

where the excited N-particle state includes the continuum state. We can then conceptually separate the excited state:

$$\psi^{N}_{EXCITED} = \psi^{N-1}_{EXCITED} + e^{-}(T)$$

The sum rule can then be derived from a consideration of the manifold of these excited "final" state ions. In the molecular case we infer the energies of these various "final" ionic states by measuring the kinetic energy of the emitted electron. The point is that this "final" state $\psi^{N}_{EXCITED}$ is not final at all; it shows time-dependent decay. This is no problem for molecules as these decay modes involve $\psi^{N-1}_{EXCITED}$ only and thus the kinetic energy of the photoelectron still reflect the energies of the quasi-final states. This is not true in solids. An excitation is created in the crystal, yielding a $\psi^{N}_{EXCITED}$; however, the system may be decaying to the ground state significantly long before the electron leaves the crystal and thus the entire $\psi^{N}_{EXCITED}$ participates in this decay. In a one-electron spirit,one would say that the initial core-hole excitation decayed (partially) into plasmons, phonons, particle-hole excitations, etc., and thus the measured kinetic energy no longer reflects that of the "quasi-final" state. It is this process of the decay of the "quasi-final state" that is described by steps 2) and 3) of the semi-classical three-step model of photoemission.

3.2 Valence Bands

The primary difference between valence band-states and core-states is that the valence band levels are describable in terms of Bloch states which extend over the entire lattice. One might therefore be tempted to conclude that there is no relaxation in the valence bands. A careful consideration of this point by Ley et al.[22] have shown this contention to be false. For a mono-valent free electron metal, (e.g. Na), the average binding energy of a valence electron relative to the vacuum level is given by

$$\overline{E_B^V} = \phi + 2/5(E_o - E_F) \quad , \qquad (3.4)$$

where ϕ is the work function, E_F the Fermi level, and E_o the bottom of the band. It is found experimentally that $\overline{E_B^V} < E_B^A$ (the atomic binding energy). In Figure 3, we note that we can write an expression for ϕ:

$$\phi = E_C + E_B^A(V) - E_R - (\bar{E}_{VB} - E_F) \quad . \tag{3.5}$$

The cohesive energy E_C appears because removing one electron breaks one bond. Approximating E_R by the localized hole picture above, one obtains very good agreement with the experimental ϕ. Comparing Eq. (3.5) with the expression obtained by Wigner and Bardeen[26] for ϕ we find

$$E_R = 0.6\ e^2/r_s - 0.458e^2/3r_s = 3.05\ \text{eV} \quad , \tag{3.6}$$

this Wigner-Bardeen result is a de-localized electron result that reflects the coulomb and exchange energy, respectively, of an *itinerant* hole propagating through the lattice. The localized-hole model yields

$$E_R = \tfrac{1}{2} \langle 3s \mid V_p \mid 3s \rangle = \tfrac{1}{2} F^0(3s,3s)_{\text{ATOMIC Na}} = 2.93\ \text{eV} \tag{3.7}$$

The near equality of these two results suggests that the relaxation energy is insensitive to the degree of localization of the initial-state.

4. CORRELATION STATES IN RARE-EARTH 4p SPECTRA

To tie several of the ideas of the previous two sections together, we present below a series of spectra for the 4p region in rare-earth metals. In these spectra the $4p_{\frac{1}{2}}$ hole state is obliterated as a single peak and appears instead as a number of well-defined individual peaks that arise through final-state correlations. With these spectra we extend to elements $Z \sim 45 - 75$ the interesting collective-resonance plus correlation effects reported by U. Gelius[7]

for elements Z = 52 - 56.

First we note that intra-shell correlation effects have shown up earlier in photoemission spectra, particularly in splitting up the lower-spin member of a multiplet such as the $3p^5 3d^5;{}^5P$ [27] or $3s^1 3p^6 3d^5;{}^5S$ [6] states in Mn^{3+}. In the latter case the formal analogy to the effect reported by Gelius is striking. The Mn^{3+} final-state is

$$3s^1 3p^6 3d^5;{}^5S$$

The two-electron excitation $p^2 \rightarrow sd$ yields

$$3s^2 3p^4 3d^5;{}^5S$$

in two ways.[6] To relate this to Gelius' spectra for Xe $4p_{\frac{1}{2}}$, the quantum numbers n and ℓ need only be raised by one, obtaining the main configuration

$$4p^5 4d^{10} 4f^0$$

and correlation states built on the configuration

$$4p^6 4d^8 4f^1$$

obtained by the excitation $d^2 \rightarrow pf$. In the relatively simple Mn^{3+} case, a sum rule is clearly operative in the spectrum, as shown in Figure 4.

For the 4p shell around Z = 54 the spectra are complicated by a collective resonance which arises through a 4p 4d 4d super Coster-Kronig transition. Gelius found that this resonance overlaps the $4p_{\frac{1}{2}}$ $4p_{3/2}$ lines for Te (Z = 52), in which the Coster-Kronig channel is energetically open. It is also well-known in x-ray spectroscopy for lighter elements down into the 4d series, and has been reported in x-ray photoemission.[28] Figure 5 shows the collective resonance in the series Z = 42 - 52. As the resonance moves up from lower binding energies, the 4p region is broadened with nearly total loss of structure. The resonance reaches the 4p

peaks at Cd (Z = 48), and gives the broadest structure at Sn (Z = 50). Gelius showed that the $4p_{3/2}$ peak emerged below the resonance (i.e., at lower binding energy) in I (Z = 53), and the $4p_{1/2}$ structure at Xe (Z = 54). This structure, which was distributed among several peaks, was also observed by Gelius in salts of Cs and Ba (Z = 55 and 56), in which the collective resonance moved progressively to higher binding energies.

Figure 6 shows the 4p region for several rare-earth metals. Final-state splitting is still clearly present in La and Ce, in fact the $4p_{1/2}$ structure closely resembles that in Cs and Ba. The structure is broadened in Ce, proabably through multiplet splitting by the 4f electron. In the other open-shell rare-earths multiplet splitting is dominant, but in Yb and Lu, at the end of the series, the $4p_{1/2}$ - $4p_{3/2}$ structure has reformed, and by Ta (Z = 73) the lines once again exhibit a simple spin-orbit doublet. This systematic behavior from Z = 42 to 73 can be understood in terms of the successive opening and closing of the 4p 4d 4d collective resonance channel and the $4d^2 \rightarrow 4p\,4f$ correlation channel. A rough idea of the origins of this behavior can be obtained from the orbital energies[29] sketched in Figure 7. Lundqvist and Wendin[30] have given a more sophisticated theoretical discussion of effects of this type.

REFERENCES

*Work done under the auspices of the U. S. Energy Research and Development Administration.

1. T. Koopmans, *Physica*, 1933, 1, 104.

2. We have neglected any differences in the correlation energy for the two states and have disregarded possible multiplet structure. They are usually small and may be of either sign; see ref. 3.

3. Relaxation in the ionic states of atoms, molecules, and solids has recently been reviewed. R. L. Martin and D. A. Shirley, "Electron Spectroscopy: Theory, Techniques, and Applications", ed. by A. D. Baker and C. R. Brundle, Academic Press, to be published.

4. J. Berkowitz, J. L. Dehmer, Y. K. Kim, and J. P. Desclaux, *J. Chem. Phys.* 1974, 61, 2556.

5. S. Süzer and D. A. Shirley, *J. Chem. Phys.* 1974, 61, 2481.

6. S. P. Kowalczyk, L. Ley, R. A. Pollak, F. R. McFeely, and D. A. Shirley, *Phys. Rev. B* 1973, 7, 4009; see also P. S. Bagus, A. J. Freeman, and F. Sasaki, *Int. J. Quant. Chem.* 1973, 7S, 83.

7. U. Gelius, *J. Electr. Spectr. and Related Phenomena* 1974, 5, 985.

8. R. L. Martin and D. A. Shirley, *J. Chem. Phys.*, in press.

9. R. L. Martin, B. E. Mills, and D. A. Shirley, *J. Chem. Phys.*, in press.

10. This is identical to a multi-determinantal extension of the sudden approximation result,[11] but comes from an application of the usual dipole approximation cross section to the satellite states.

11. T. Åberg, *Phys. Rev.* 1967, 156, 35.

12a. Even at this preliminary stage, however, certain points are evident. For example, we corroborate the earlier assignment (see ref. 12b) of the first four satellites as $(2p \rightarrow 3p)_{lower}$, $(2p \rightarrow 3p)_{upper}$, $(2p \rightarrow 4p)_{lower}$, and $(2p \rightarrow 5p)_{lower}$.

We furthermore predict the state $(2p \rightarrow 6p)_{lower}$ to occur at a relative energy of 44.2 eV, in agreement with Gelius' assignment of state 5. Its partner, $(2p \rightarrow 6p)_{upper}$, lies at ΔE = 48.4 eV. This state is calculated to have a very small intensity and was not observed by Gelius. The assignment of the peaks at 59.6 and 65.9 eV as involving $2s \rightarrow 3s$ excitations is given support by the calculations. We also find the $(2s \rightarrow 4s)_{lower}$ state to fall in this region with an unobservable intensity. Examination of Table 2 shows that the $(2p \rightarrow np)_{lower}$ states form a very definite Rydberg progression leading to the $1s^1 2s^2 2p^5 (^3P)$ shake-off limit 45.2 eV from the Ne 1s primary state. The $(2p \rightarrow np)_{upper}$ states converge to the ^1P shake-off limit at 49.5 eV.

12b. The assignment was made with the help of multi-configuration Hartree-Fock calculations by P. S. Bagus and U. Gelius reported in K. Siegbahn, C. Nordling, G. Johannson, J. Hedman, P. F. Hedén, K. Hamrin, U. Gelius, T. Bergmark, L. O. Werme, R. Manne, and Y. Baer, ESCA Applied to Free Molecules, North-Holland, Amsterdam, 1969.

13. R. Manne and T. Åberg, *Chem. Phys. Letters* 1970, 7, 282.

14. G. D. Mahan, *Phys. Rev. B* 1970, 2, 4334.

15. P. J. Fiebelman and D. E. Eastman, *Phys. Rev. B* 1974, 10, 4932.

16. L. Hedin and G. Johannson, *J. Phys. B* 1969, 2, 1336.

17. J. Friedel, *Advan. Phys.* 1954, 3, 446.

18. P. H. Citrin, *Phys. Rev. B* 1973, 8, 5545.

19. S. Hüfner, G. K. Wertheim, D. N. E. Buchanan, and K. W. West, *Phys. Letters A* 1974, 46, 420.

20. G. D. Mahan, *Phys. Rev.* 1967, 163, 612.

21. P. W. Anderson, *Phys. Rev. Letters* 1967, 18, 1049; *Phys. Rev.* 1968, 164, 352.

22. L. Ley, F. R. McFeely, S. P. Kowalczyk, J. G. Jenkin, and D. A. Shirley, *Phys. Rev. B* 1975, 11, 600.

23. L. Hedin, B. I. Lundqvist, and S. Lundqvist, *Solid State Commun.* 1967, 5, 237; B. I. Lundqvist, *Phys. Kondensierten Materie* 1969, 9, 236.

24. D. C. Langreth, *Phys. Rev. B* 1970, 1, 471.

25. R. A. Pollak, L. Ley, F. R. McFeely, S. P. Kowalczyk, and D. A. Shirley, *J. Electr. Spectr.* 1974, 3, 381.

26. E. Wigner and J. Bardeen, *Phys. Rev.* 1935, 48, 84.

27. C. S. Fadley, D. A. Shirley, A. J. Freeman, P. S. Bagus, and J. V. Mallow, *Phys. Rev. Letters* 1969, 23, 1397; S. P. Kowalczyk, L. Ley, F. R. McFeely, and D. A. Shirley, *Phys. Rev. B* 1975, 11, 1721.

28. G. B. Fisher, R. Shalovy and P. J. Estrup, *Bull. Amer. Phys. Soc. Ser. II* 1974, 19, 233.

29. C. C. Lu, T. A. Carlson, F. B. Malik, T. C. Tucker, and C. W. Nestor, *Atomic Data* 1971, 3, 1.

30. S. Lundqvist and G. Wendin, *J. Electr. Spectros.* 1974, 5, 513.

TABLE 1. HF satellite peak intensities in the overlap approximation.[a)]

State[b]	Description[c]	Method A I_n(theo)[d]	Method B I_n(theo)[d]	I_n(expt)[e]	E(theo)[f]	E(expt)[f]
0	$1\sigma^1 2\sigma^2 3\sigma^2 1\pi^4$	(100.0)	(100.0)	(100.0)	693.5	694.0(5)
1	$(3\sigma \rightarrow 4\sigma)_{lower}$	0.0	0.1	--	23.89	--
2	$(3\sigma \rightarrow 4\sigma)_{upper}$	1.2	2.0	1.9(3)	25.90	22.4(2)
3	$(1\pi \rightarrow 2\pi)_{lower}$	1.5	3.0	3.0(4)	29.57	26.50(9)
4	$(3\sigma \rightarrow 5\sigma)_{lower}$	0.0	0.0	--	30.89	--
5	$(1\pi \rightarrow 2\pi)_{upper}$	3.6	6.2	5.7(5)	32.35	29.90(7)
6	$(1\pi \rightarrow 3\pi)_{lower}$	0.0	0.1	--	32.72	--
7	$(3\sigma \rightarrow 5\sigma)_{upper}$	0.7	1.2	1.0	33.31	30.87
8	$(3\sigma \rightarrow 6\sigma)_{lower}$	0.0	0.0	--	33.74	--
9	$(1\pi \rightarrow 4\pi)_{lower}$	2.8	4.1	3.8(5)	34.84	32.7(3)
10	$(3\sigma \rightarrow 7\sigma)_{lower}$	0.5	0.7	0.7	35.43	33.3
11	$(1\pi \rightarrow 3\pi)_{upper}$	0.0	0.0	--	35.72	--

[a]From ref. 9.

[b]In order of increasing energy.

[c]The descriptions are somewhat oversimplified. In many of the states configurations with a large overlap with the initial state have very small coefficients but supply relatively large contributions to the computed intensity.

The 3σ orbital in HF is the bonding combination of $F(2p_\sigma)$ and H(1s), while the 1π orbital is $F(2p_\pi)$. The virtual orbitals are roughly described as follows: 4σ - antibonding combination of $F(2p_\sigma)$ and H(1s); 5σ - F(3s); 6σ - $F(3p_\sigma)$; 7σ - $F(3d_\sigma)$; 2π - $F(3p_\pi)$; 3π - $F(3d_\pi)$; 4π - $F(4p_\pi)$.

[d]All intensities are normalized to peak 0. Absolute values of $(S_0^{11})^2$ are 0.781 (Method A) and 0.720 (Method B).

[e]Error in last place given parenthetically

[f]The first entry is the absolute binding energy of the F 1s hole state in eV; the others are incremental energies relative to this.

TABLE 2. Preliminary results for the Ne 1s satellite intensities.

State	Description	I_n(theo)[a]	I_n(expt)[b]	E(theo)[c]	E(expt)[d]
0	$1s^1 2s^2 2p^6$	(100.0)	(100.0)	(868.6)	(870.4)
1	$(2p \rightarrow 3p)_{lower}$	1.32	3.15(8)	36.8	37.35(2)
2	$(2p \rightarrow 3p)_{upper}$	1.43	3.13(10)	40.0	40.76(3)
3	$(2p \rightarrow 4p)_{lower}$	1.13	2.02(10)	41.6	42.34(4)
4	$(2p \rightarrow 5p)_{lower}$	0.34	0.42(6)	43.3	44.08(5)
5	$(2p \rightarrow 6p)_{lower}$	0.10	$\sim .2^*$	44.2	45.10(7)
6	$1s^1 2s^2 2p^5 (^3P)$	--	--	45.2	47.4 (5)
7	$(2p \rightarrow 4p)_{upper}$	0.49	0.96(11)	45.5	46.44(5)
8	$(2p \rightarrow 5p)_{upper}$	0.13	0.17(5)	47.4	48.47(7)
9	$(2p \rightarrow 6p)_{upper}$	0.04	--	48.4	--
10	$1s^1 2s^2 2p^5 (^1P)$	--	--	49.5	51.7 (5)
11	$(2s \rightarrow 3s)_{lower}$	0.09	0.57(5)	61.3	59.8 (1)
12	$(2s \rightarrow 4s)_{lower}$	0.00	--	68.2	--
13	$(2s \rightarrow 3s)_{upper}$	0.16	0.49(6)	68.4	65.9 (1)
14	$(2s \rightarrow 5s)_{lower}$	0.00	--	70.8	--
15	$(2s \rightarrow 4s)_{upper}$	0.02	--	75.7	--

[a] Based on Method A, see text.

[b] From ref. 7. The starred entry, (state 5), is an approximation we have made from visual inspection of the spectrum in ref. 7. Gelius reports an intensity of 0.50(15), which we feel must be a misprint.

[c] The first entry is the computed Ne 1s binding energy in electron volts; all others are incremental relative to this.

[d] From ref. 7.

FIGURE CAPTIONS

Fig. 1. Typical photoemission spectrum of a metal valence band (top) and of a metal core level (bottom). (After ref. 22.)

Fig. 2. Experimental excess metallic binding energies based on an atomic orbital approximation to the screening state, using the model described in text (after ref. 3). Note the drop in extra-atomic relaxation energy in Cu and Zn which reflects the loss of 3d-screening due to the filling of the 3d-band.

Fig. 3. Energy level diagram relating the binding energy of a 3s electron in atomic Na to that of a 3s electron in the metal valence band (after ref. 22).

Fig. 4. (a) Schematic representation of the one-electron (Koopmans' Theorem) spectrum for the Mn^{3+} $3s^1 3p^6 3d^5$ final-state.

(b) Schematic representation of the observed spectrum of the Mn 3s region in MnF_2 (after ref. 6). This illustrates the partitioning of energy and intensity through the sum rule. The satellites labeled ^5S' are correlation states arising from strong interaction of the $3s^2 3p^4 3d^6$ configuration with the $3s^1 3p^6 3d^5$ final-state.

Fig. 5. Left panel shows the XPS spectra of the 4s 4p region of the metals Mo (Z = 42) - Ag (Z = 47). Right panel shows XPS spectra of the 4s 4p region of the elements Cd (Z = 48) - Te (Z = 52) which exhibit the strong collective resonance discussed in the text.

Fig. 6. The XPS spectra of the 4p region of La (Z = 57), Ce (Z = 58), Yb (Z = 70), Lu (Z = 71), and Ta (Z = 73) metals. La and Ce exhibit correlation states of the type discussed in Section 4. Yb and Lu, where the $4d^2 \rightarrow 4p\,4f$ correlation channel becomes closed with the filling of the 4f shell, shows both $4p_{1/2}$ and $4p_{3/2}$ levels. These levels, however, also have a satellite. Ta displays just spin-orbit splitting.

Fig. 7. Orbital energies from ref. 29, illustrating final-state effects in the 4p shell. Energy for I ($Z = 53$) is adjusted to fit data of Gelius. In Region I the collective resonance coincides with 4p states, because $\varepsilon(4p) + \varepsilon(4f) \sim 2\varepsilon(4d)$. In Region II the same condition is met, but the $d^2 \rightarrow pf$ excitation yields a bound state, hence discrete shake-up lines. This structure is obscured for $Z > 58$ by multiplet splitting. The 4f channel is closed for $Z > 70$ and the simple $4p_{1/2} - 4p_{3/2}$ structure is restored by $Z = 73$.

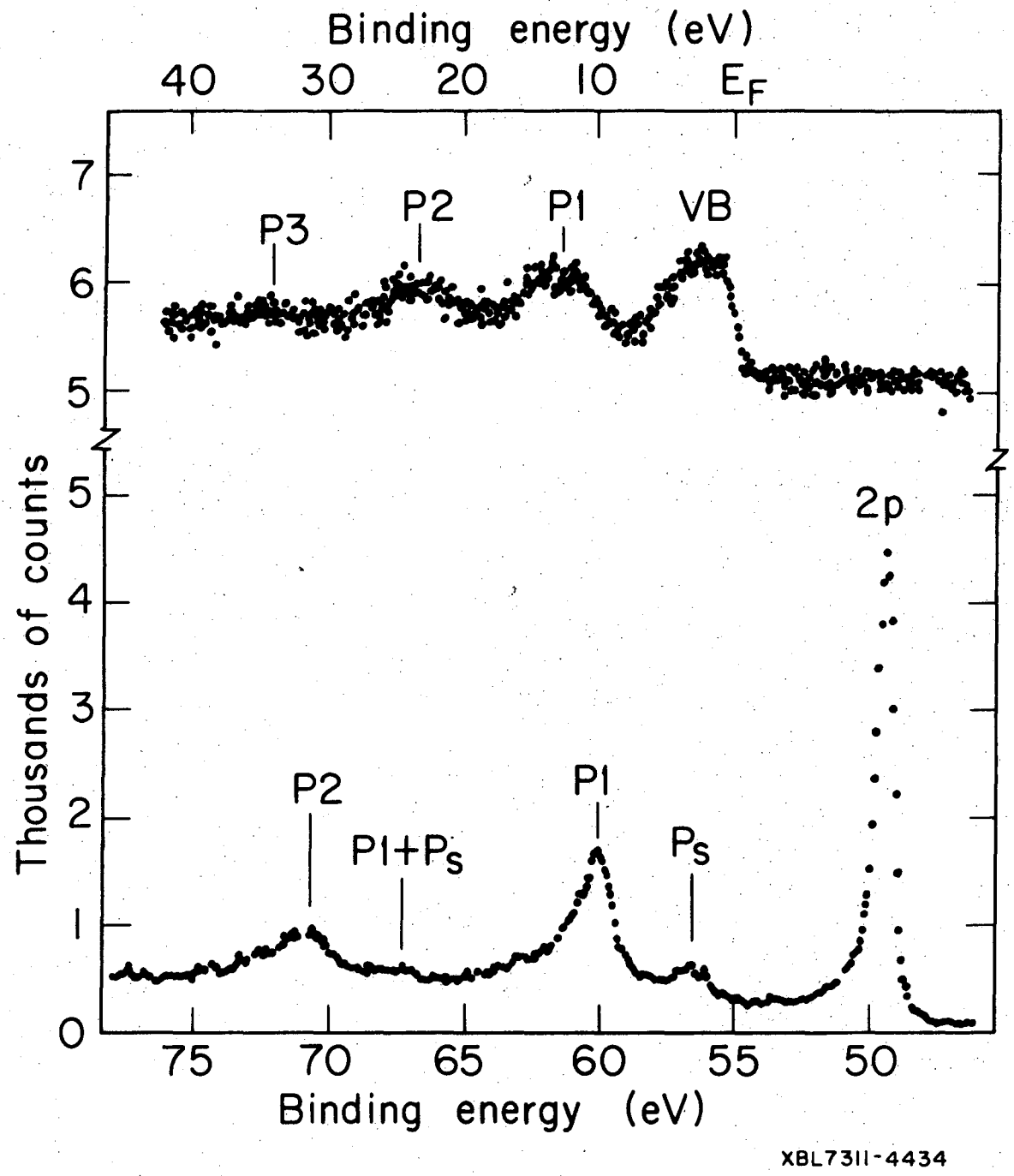

Fig. 1.

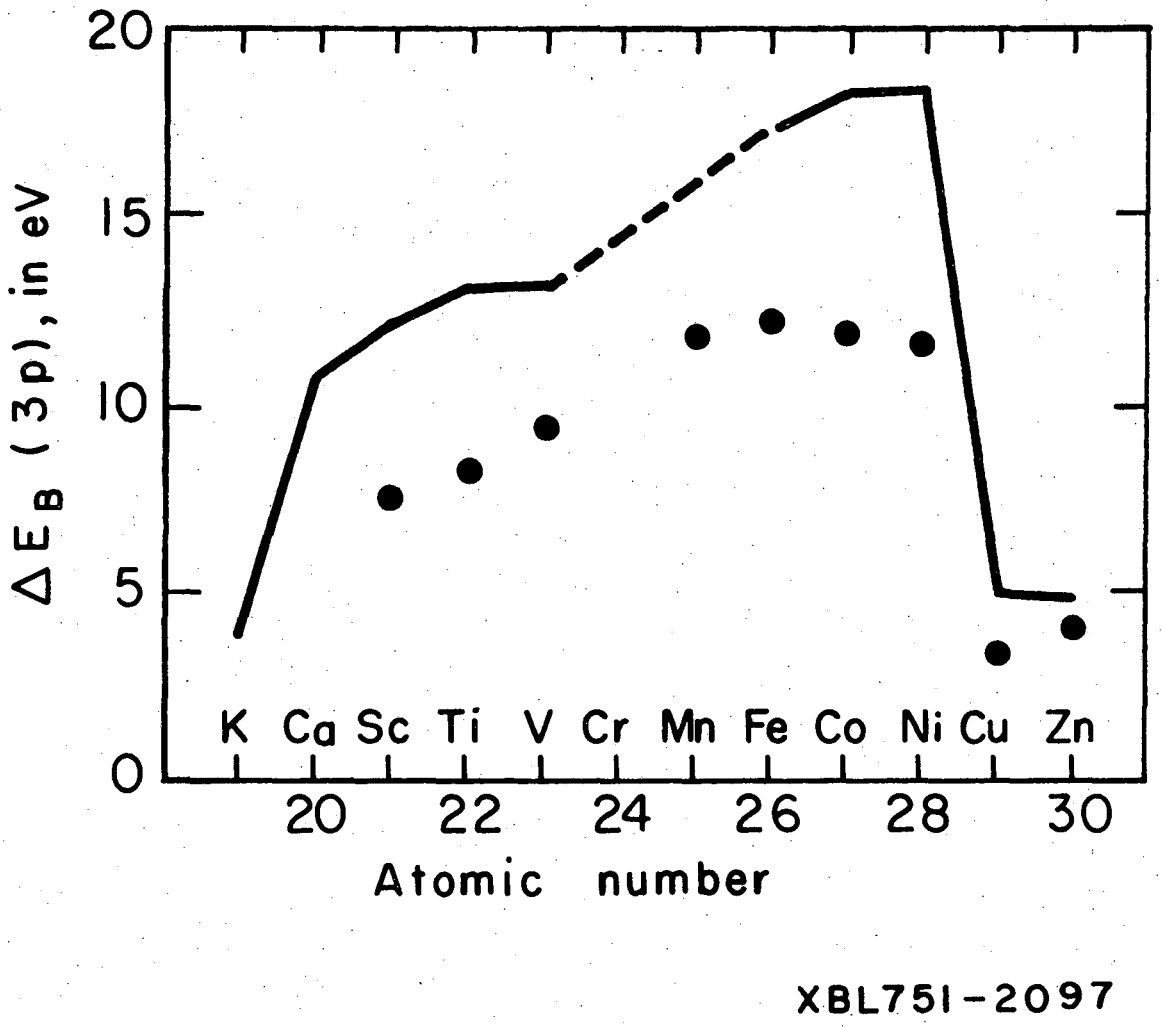
20
15
10
5
0
ΔE_B (3p), in eV
K Ca Sc Ti V Cr Mn Fe Co Ni Cu Zn
20 22 24 26 28 30
Atomic number
XBL751-2097

Fig. 2.

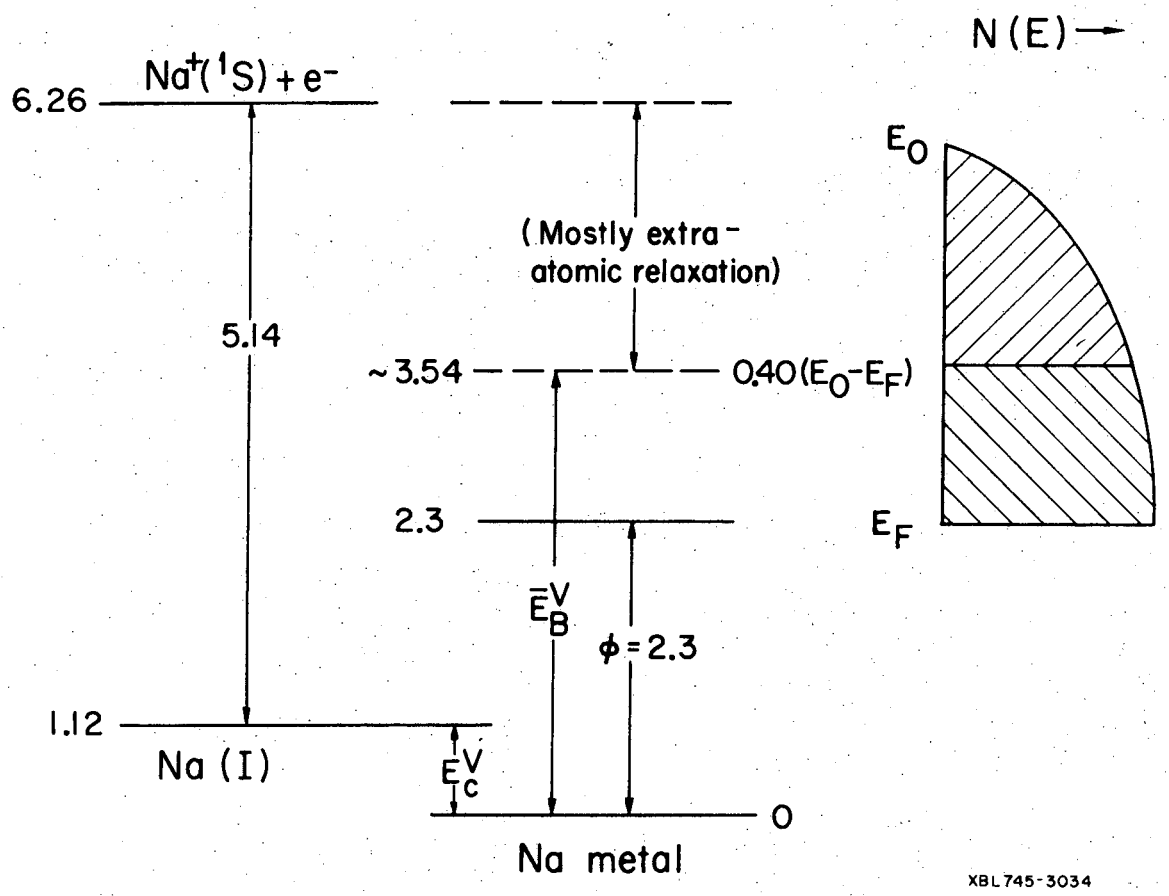

Fig. 3.

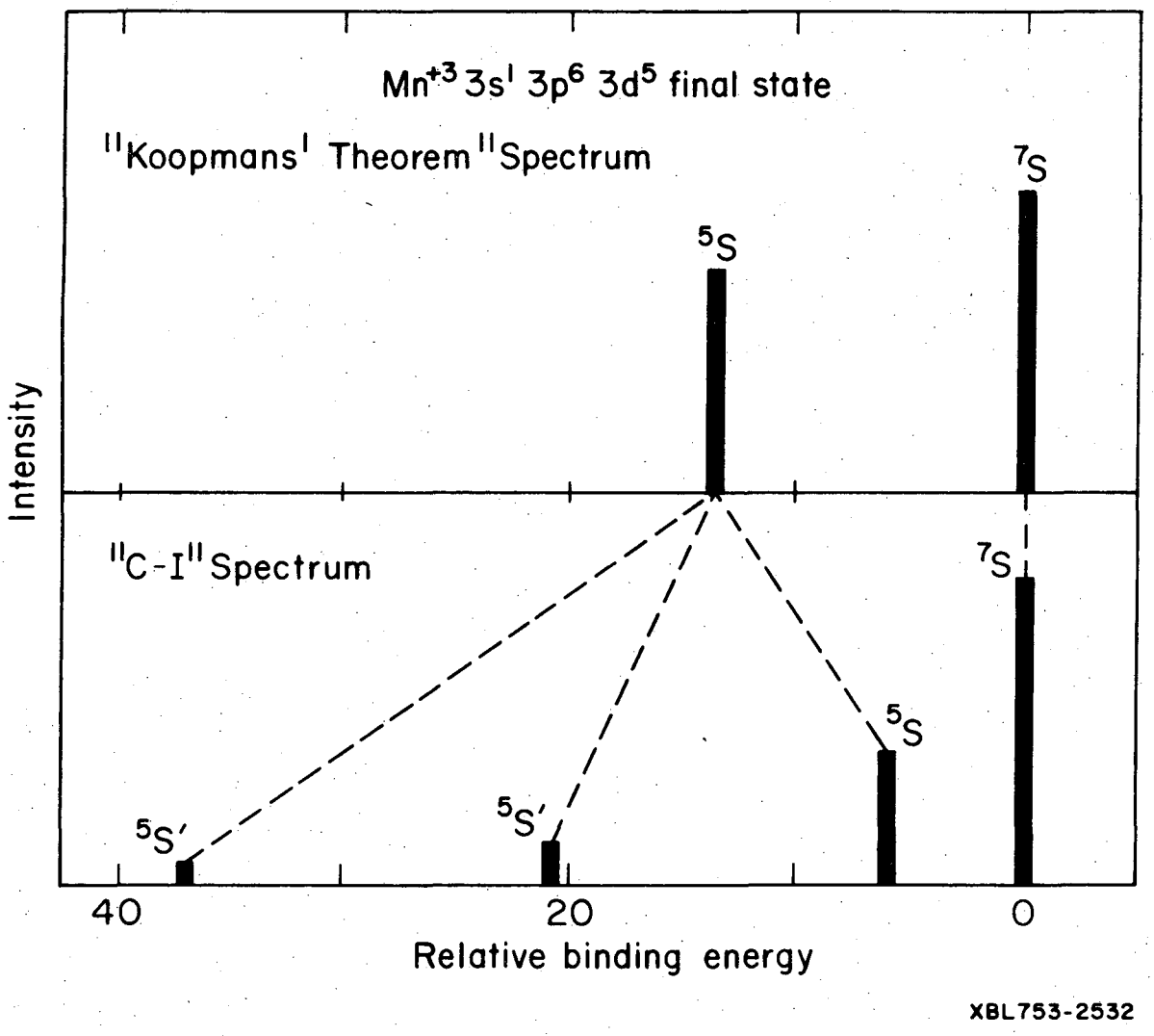
Mn+3 3s1 3p6 3d5 final state
"Koopmans' Theorem" Spectrum
7S
5S
Intensity
"C-I" Spectrum
7S
5S
5S'
5S'
40
20
0
Relative binding energy
XBL753-2532

Fig. 4.

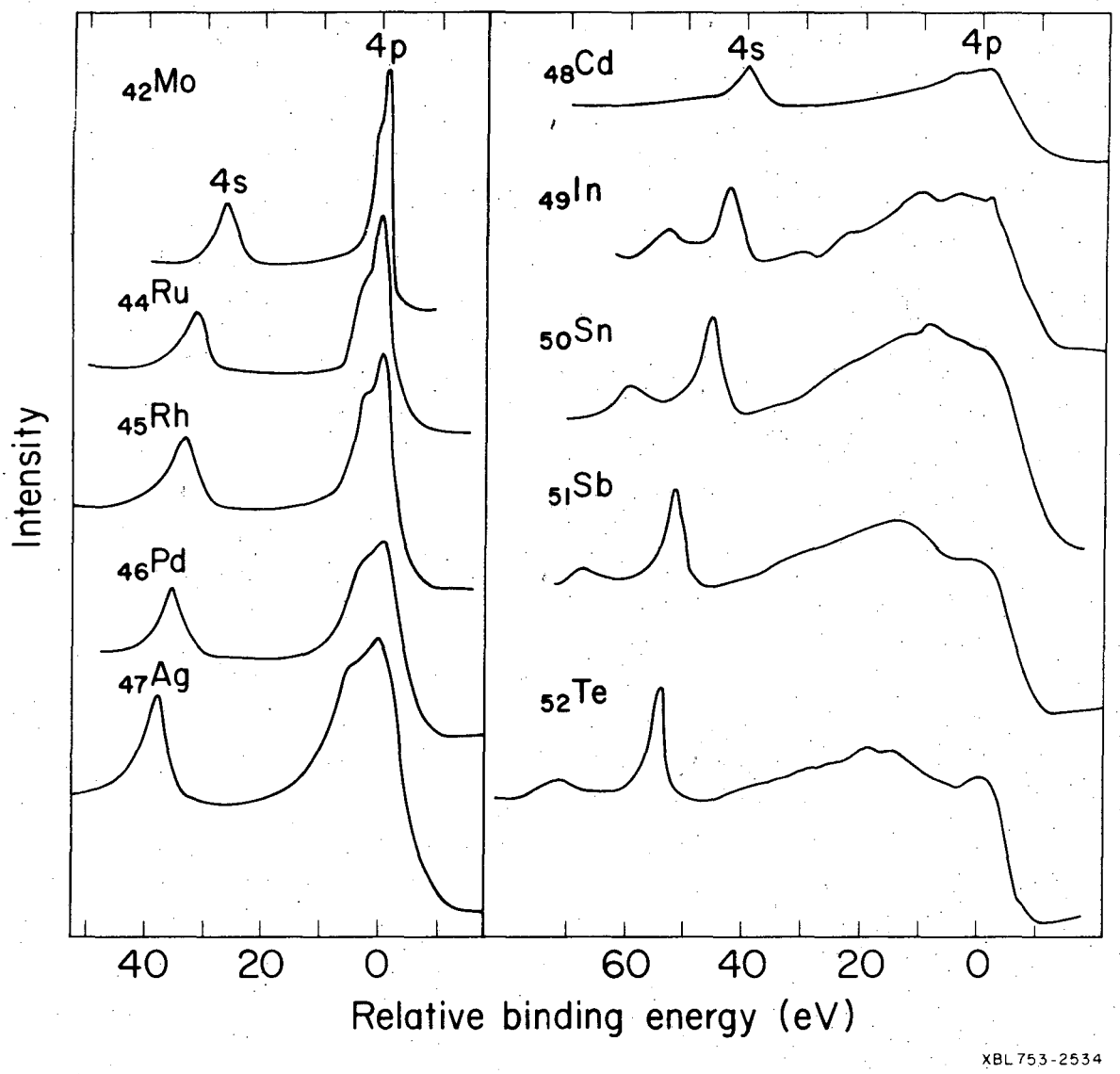

Fig. 5.

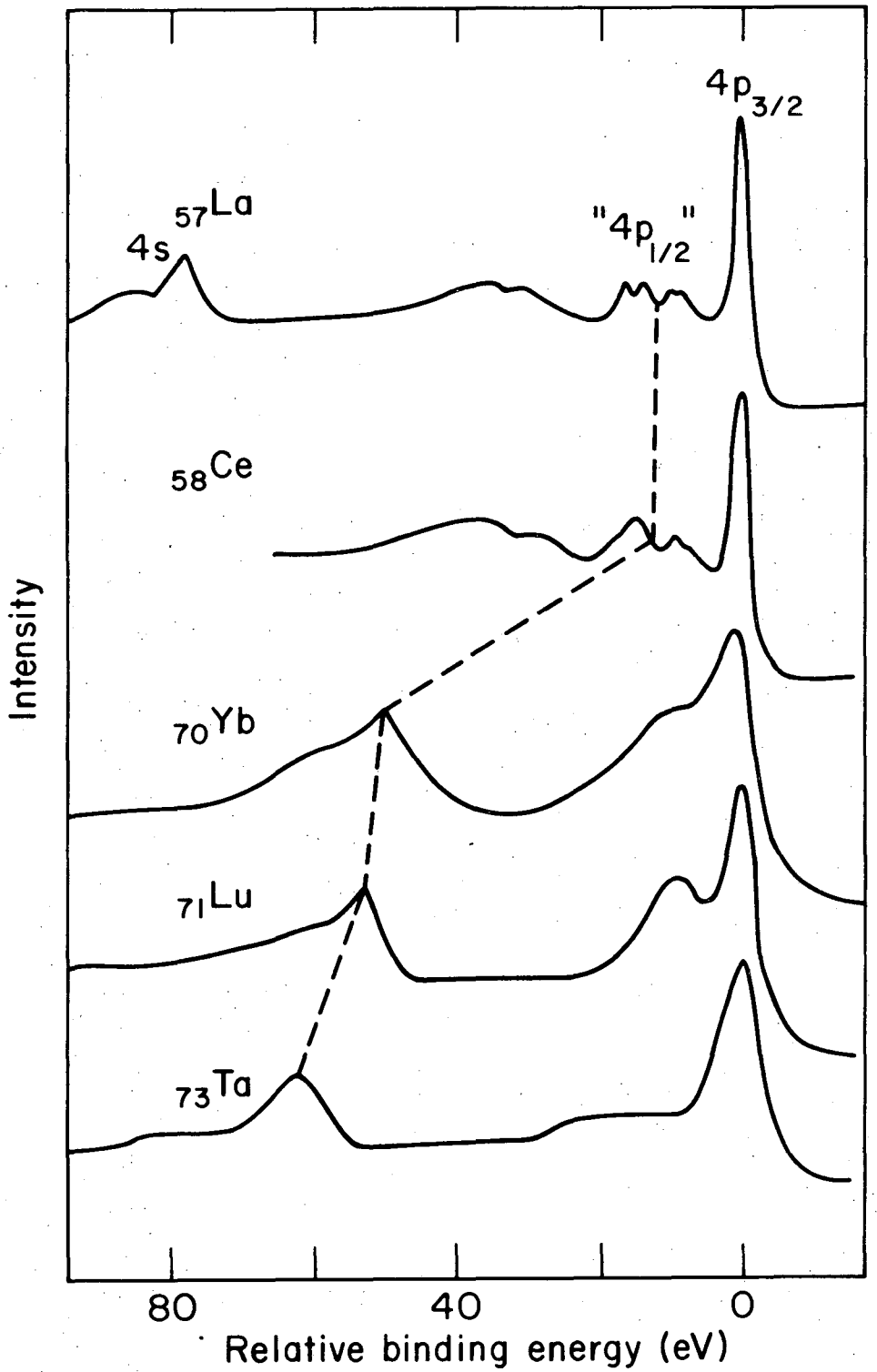
4p3/2
57La
4s
"4p1/2"
58Ce
Intensity
70Yb
71Lu
73Ta
80
40
0
Relative binding energy (eV)
XBL 753-2533

Fig. 6.

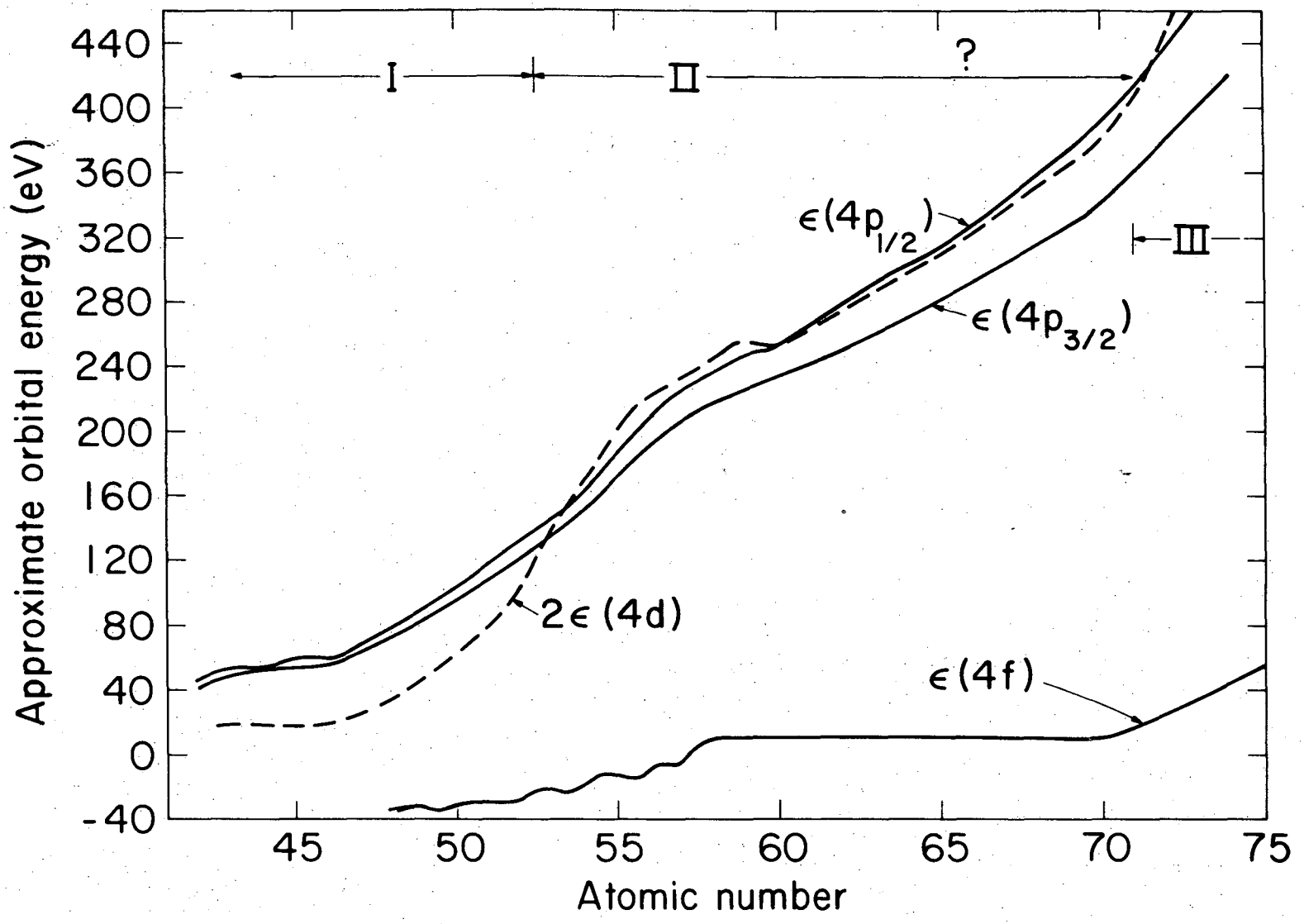

Fig. 7

TECHNICAL INFORMATION DIVISION
LAWRENCE BERKELEY LABORATORY
UNIVERSITY OF CALIFORNIA
BERKELEY, CALIFORNIA 94720